UNIVERSITY OF CALIFORNIA SAN DIEGO

The Role of Dimerization of PTPRA in Fibroblast Like Synoviocytes

A thesis submitted in partial satisfaction of the requirements for the degree Master of Science

in

Biology

by

Daniel Woei Koung Lee

Committee in charge:

Professor Nunzio Bottini, Chair
Professor Eric Allen, Co-Chair
Professor Joseph Pogliano

2019

The thesis of Daniel Woei Koung Lee is approved, and it is acceptable in quality and form for publication on microfilm and electronically:

Co-chair

Chair

University of California San Diego

2019

Dedication

To my parents

Kenneth and Marilyn Lee

TABLE OF CONTENTS

LIST OF FIGURES

ACKNOWLEDGMENTS

I would like to acknowledge Professor Nunzio Bottini as the chair of my committee, whom without I would never have had the opportunity to perform this study.

I would also like to acknowledge Dr. Dennis Wu for mentoring me in my time in the Bottini Lab.

I would also like to acknowledge Dr. William Kiosses of La Jolla Institute of Immunology, who handled all image acquisitions and taught me much about microscopy and analysis.

ABSTRACT OF THE THESIS

The Role of Dimerization of PTPRA in Fibroblast Like Synoviocytes

by

Daniel Woei Koung Lee

Master of Science in Biology

University of California, San Diego, 2019

Professor Nunzio Bottini, Chair

Professor Eric Allen, Co-chair

Rheumatoid arthritis is a chronic, progressive autoimmune disease in which fibroblast like synoviocytes (FLS) play a key role. In the pathogenesis of the disease, FLS infiltrate the joints and promote inflammation and destruction of joint cartilage. Tranmembrane protein tyrosine phosphatase receptor type alpha (PTPRA), a known activator of the kinase Src, is highly expressed in RA FLS and promotes their aggressiveness. Knockout of PTPRA protects against joint swelling and disease

progression in KBxN models of mice arthritis. A canonical model of transmembrane PTP regulation is that they are inactivated by dimerization. However, these models were never validated by single cell assessments of full length PTPs in primary cells. Here, through FRET microscopy and functional assays of multiple independent primary PTPRA knockout murine FLS cell lines transfected with PTPRA mutant constructs, we show that PTPRA dimerization occurs in FLS and positively correlates with PTPRA association with Src and promotion of cell motility. PTPRA mutants impairing dimerization of PTPRA and its association to Src at the leading edge of migrating mouse FLS also displayed impaired cell morphology and motility. These results are apparently inconsistent with the aforementioned canonical model of transmembrane PTP regulation, indicating the need for further investigations of PTPRA regulation.

Introduction

Rheumatoid arthritis (RA) is a debilitating autoimmune disease affecting 1.5 million Americans characterized by immune-driven chronic inflammation, destruction of joint tissue, and, eventually, bone erosion and joint deformity (Myasoedova et al., 2010). It is a chronic, systemic disease which can lead to permanent damage and reduced patient quality of life, and modern treatment consists of early, aggressive immunosuppressive action to stop inflammation and slow disease progression (Smolen, Aletaha, & McInnes, 2016). The chronic and progressive nature of the disease if left untreated highlights the importance of developing new treatments for the >30% patients who display an incomplete response to available medications (Rubbert-Roth & Finckh, 2009). Previous research by Dr. Stanford in the Bottini laboratory has demonstrated that the transmembrane protein tyrosine phosphatase receptor type alpha (PTPRA) is highly expressed in arthritic mouse joints, particularly in fibroblast like synoviocytes (FLS), and that PTPRA knock out (KO) mice are protected from joint swelling and disease progression in KBxN models of mice arthritis (Stanford et al., 2016). FLS are joint-lining non immunological cells which normally contribute to maintain the normal structure of the synovium. However, in RA, FLS acquire an invasive and aggressive behavior and contribute to the destructive action of the inflammatory tissue (called “pannus”) that infiltrates the joint. FLS play both a “passive responder” -subjected to stimulations by the pro-inflammatory milieau of the arthritic joints- and “imprinted aggressor” -secondary to epigenetic changes that enhance their destructive action- role in RA (Bottini & Firestein, 2013). FLS are a major component of the hyperplastic infiltrating inflammatory tissue -called pannus- that characterizes RA and through infiltration, reduced apoptosis,

and the secretion of proinflammatory cytokines and matrix metalloproteinases, they promote the degradation of the cartilage lining in the joint (Bottini & Firestein, 2013). Finding a method to limit the pathogenic activity of FLS in RA pannus could prove useful in slowing down the progression of disease especially if novel anti-FLS agents can be combined with immunosuppressive medications.

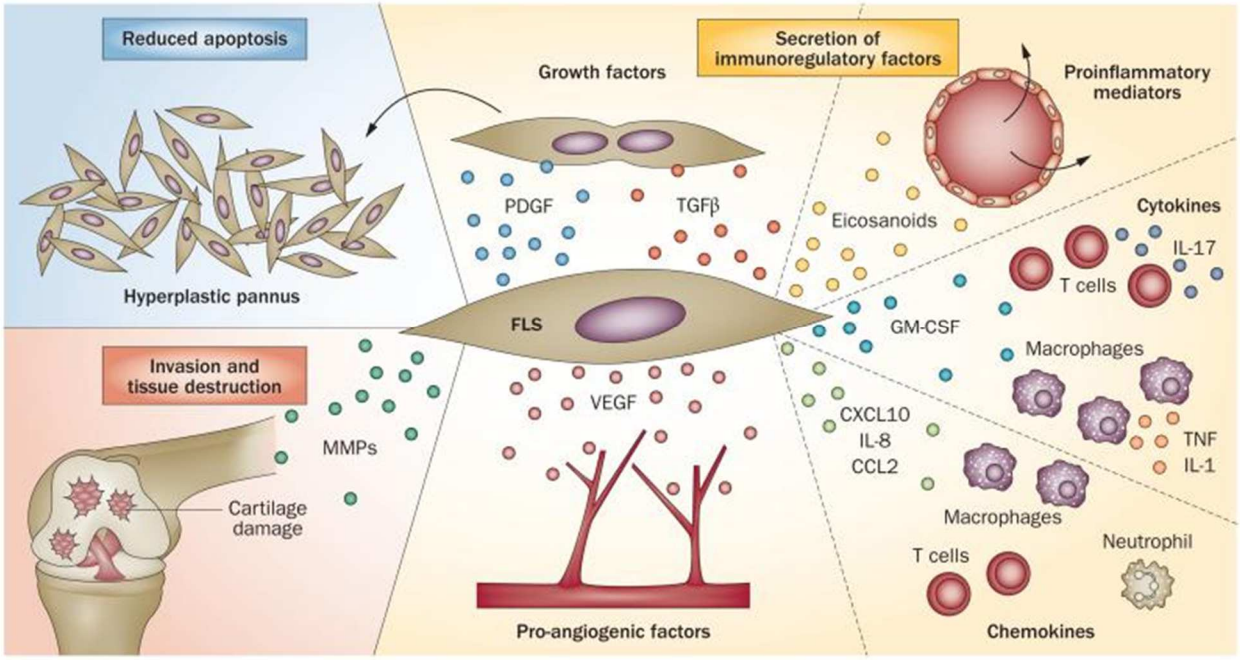

Figure 1. Roles of FLS in RA. FLS in the rheumatoid joint are inflammation-driven but also display an imprinted aggressive phenotype that is persistent in ex vivo cultures. Reprinted with permission from Bottini et al, 2012

Dr. Stanford's work showed that PTPRA promotes Src kinase-dependent cell signaling and motility in FLS, amplifying their proinflammatory and invasive action (Stanford et al., 2016). Src is a well-known protein tyrosine kinase that co-activates with the focal adhesion kinase (FAK) to regulate cell signaling, motility, and proliferation (Herrera Abreu et al., 2008). The FAK-Src complex is known to mediate the invasive phenotype of cancer cells and is suspected to play a similar role in RA FLS. Elucidating the role and mechanism of action of PTPRA in regulating the activation of Src could

reveal possible approaches for reducing Src activity in RA FLS, and subsequently the RA FLS hyperplasticity and invasiveness in RA pannus.

Previous work by Dr. den Hertog has shown that PTPRA dimerizes in biochemical assays and it has been proposed that dimerization reduces the function of PTPRA (Blanchetot, Overvoorde, & den Hertog, 2003). Indeed the canonical model of transmembrane PTP regulation -mostly built upon observations made on PTPRA- dictates that these enzymes are deactivated via switch to a dimerized, inactive state and are activated when switched back to a monomeric state (Jiang, den Hertog, & Hunter, 2000). Despite the fact that the published observations about PTPRA fit such canonical model, dimerization of PTPRA and its effects on PTPRA activity regulation have not yet been observed/assessed in primary cells by microscopy or other cellular biology approaches. Assays performed in vitro with lysed cells might not be representative of conditions within living cells, and both dimerization and activity of PTPRA could be altered when cells are lysed. The den Hertog laboratory has reported a fluorescence resonance energy transfer (FRET) analysis of in SK-N-MC neuroepithelioma cells expressing CFP/YFP fusion proteins of PTPRA which also suggested dimerization of PTPRA in these cells, but the fusion proteins utilized were truncation mutants and the behavior of PTPRA in cancer cell lines might not be representative of its physiology in primary fibroblasts (Tertoolen et al., 2001). In addition, nothing is known about the dimerization's role in regulating PTPRA downstream physiological functions.

The goal of my work in the Bottini laboratory was to further elucidate the role of dimerization in the function of PTPRA using primary FLS, and assess whether

dimerization could possibly be a targetable mechanism to modulate the behavior of FLS in RA. The methods of choice were FRET microscopy experiments and functional assays in PTPRA knock out (KO) FLS reconstituted with wild type (WT) or mutants of PTPRA.

PTPRA includes (see also **Fig. 2**) 1) two intracellular phosphatase domains (D1 and D2) - of which the membrane proximal D1 is catalytically active, while the membrane distal D2 has been reported to regulate PTPRA dimerization-, 2) a juxtamembrane portion including a so called “wedge” domain- which mediates dimerization by interacting with the active site of other PTPRA monomers, 3) a transmembrane domain, and 4) a small heavily glycosylated extracellular domain (Tonks, 2006). We were interested primarily in showing that dimerization occurs in FLS and assess how it regulates the function of PTPRA. We created three PTPRA mutants: P210L/P211L, a construct which includes two point mutations in the juxtamembrane portion previously discovered to reduce dimerization; dD2, a construct completely missing the less catalytically active D2 domain; and dEC, which is missing the extracellular domain. P210L/P211L was first used by the den Hertog laboratory as a dimerization-deficient mutant. The point mutations disrupt the ability of the wedge domain of PTPRA to lodge itself into the D1 domain of another PTPRA molecule, which Hertog theorized to lead to a dimerized, inactive state since the wedge domain would block access to the catalytic cysteine in the D1 domain (Jiang, den Hertog, & Hunter, 2000). dD2 and dEC were also theorized to play a role in PTPRA dimerization, though it is not currently understood how exactly they perform such a role (Jiang, den Hertog, & Hunter, 2000).

In this study, PTPRA dimerization and interaction with Src was determined by FRET between PTPRA constructs, labeled with either FLAG or HA tags, or between PTPRA and Src. FRET is the transfer of energy from one excited fluorophore to another fluorophore in close proximity, less than 10 nanometers, through long range dipole-dipole coupling (Shrestha et al., 2015). A positive FRET signal is suggestive of dimerization or association between the proteins to which the fluorophores are attached, and FRET microscopy can be utilized to determine the % of dimerization/association and localization of dimers/complexes within the cell. Through the optimization of a scratch wound healing assay that models pathological migration of FLS in RA, we could generate and image a leading edge of migrating FLS, and in strict collaboration with Dr. William Kiosses at the La Jolla Institute for Immunology, who is an expert in the FRET-based microscopy approach, we could use FRET to study PTPRA's dimerization and its association with Src.

Microscopy data was then backed up through functional motility assays of FLS transfected with the different constructs to correlate the effect of PTPRA dimerization with its regulation of FLS invasiveness. I utilized a wound healing scratch assay similar to the assay used for microscopy, but the focus was on measuring physical wound closure rate rather than localization and complex formation of PTPRA within individual cells along the wound's edge. I also performed transwell migration assays, where cells were allowed to migrate through a permeable membrane towards serum rich media acting as a chemotactic stimulus.

In the following pages I will present the results of the above-mentioned assays. The project will continue using more advanced FRET techniques in order to verify the

already obtained findings. In addition, there are other potential phenotypes dependent on PTPRA that can be further studied in relation to dimerization to support any model emerging from these initial studies.

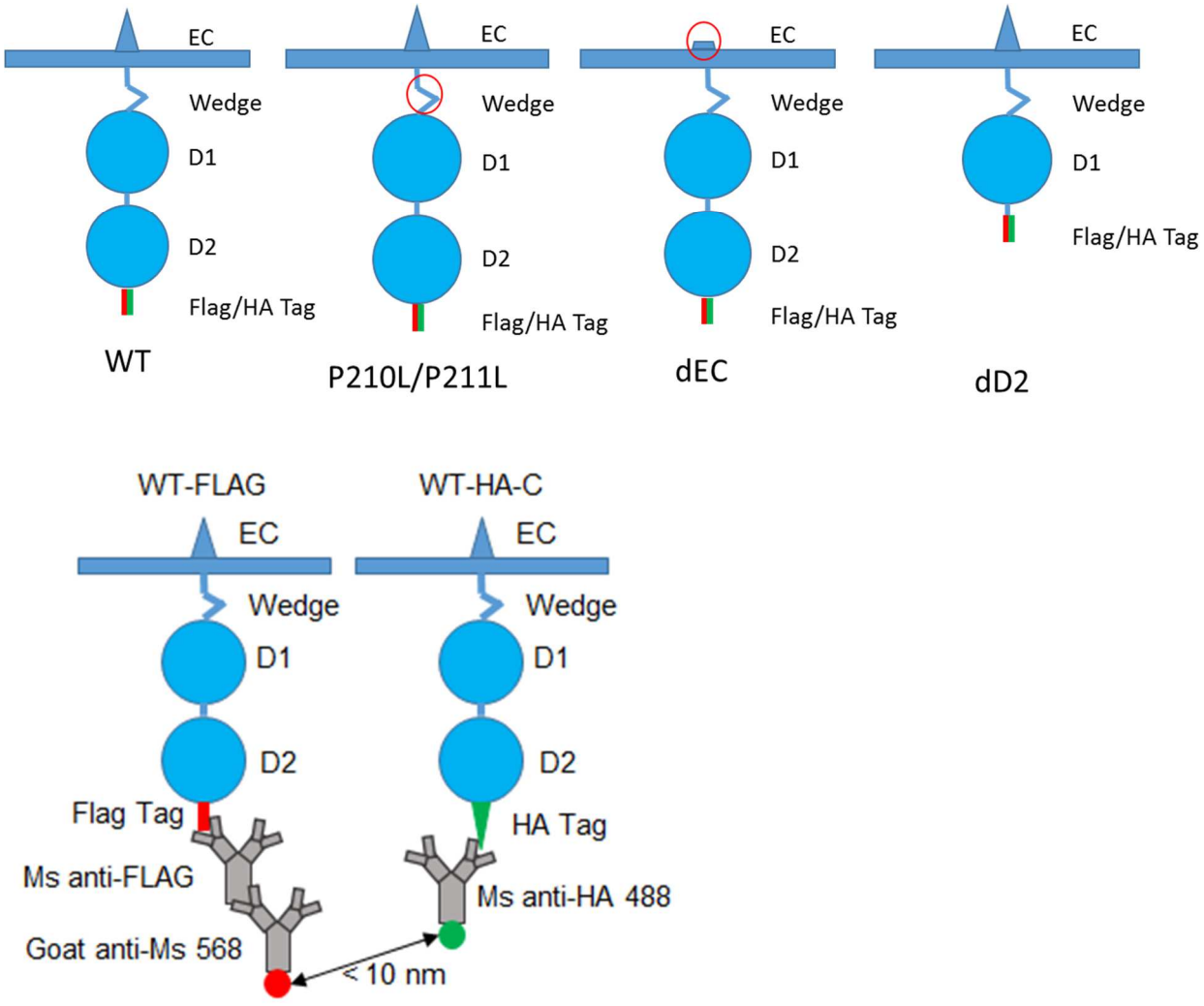

Figure 2. A scheme of our PTPRA mutant constructs, and protocol and mechanism of FRET occurrence

Methods

Antibodies:

Primary:

Mouse anti-Flag F3165 (Sigma Aldrich)

Rabbit anti-Src 2108S (Cell Signaling)

Secondary:

Goat anti-Mouse Alexa 568 A11031 (Invitrogen)

Goat anti-Rabbit Alexa 488 A11008 (Invitrogen)

Direct Conjugates:

Mouse anti-HA Alexa 488 2350S (Cell Signaling)

Mouse Fibroblast like Synoviocytes

For mouse FLS lines, knee and ankle joints were isolated from 8-week old Ptpra WT and KO littermate pairs. Minced tissues were digested in 0.5 mg/ml collagenase IV in RPMI for 2 h at 37°C with gentle agitation and cultured for 4 days in FLS media (DMEM (Fishersci 10-017) containing 10% fetal bovine serum (FBS; Omega Scientific), 2 mM L-glutamine, 100 units/ml penicillin, 100 g/ml streptomycin and 50 microg/ml gentamicin (Life Technologies) at 37°C in a humidified 5% CO2 atmosphere. Lines were used for assays between the 3rd and 10th passage, and after overnight starvation in 0.1% FBS (serum-starvation media).

Cell Culture and Transfection

Cells were grown in media containing DMEM (Fishersci 10-017), 10% fetal bovine serum (FBS; Omega Scientific), 2mM L-glutamine, 100 units/ml penicillin, 100 g/ml streptomycin and 50 microg/ml Gentamicin (Life Technologies) at 37°C in a humidified 5% CO2 atmosphere. Transfection was performed using Invitrogen Lipofectamine 3000 once monolayer reached approximately 90% confluency. The transfection media was DMEM 10-017 with no additional additives, replaced with normal FLS media 3 hours post transfection. For assays, cells were starved for 12 h 36 h post transfection using 0.1% serum media.

Western Blotting

Cells were lysed with a high SDS denaturing buffer (1x Laemmli sample buffer, 5% bME, 2.05% SDS) and the gel was transferred at 40 volts at 60 °C for 1.5 h. Primary antibodies were diluted 1:1000 and secondary antibodies were diluted 1:5000.

Plasmids

Plasmids were ordered from GenScript. Wildtype PTPRA (NM_008980.2) was cloned into a pcDNA3.1 (+) backbone between the AflII and XhoI restriction sites and were expressed in both C-terminal FLAG and HA tag variants. The P210L/P211L mutant construct contains two proline to leucine point mutations in the wedge domain of the juxtamembrane portion. dD2 contains a deletion between aa 560-818 corresponding to the less catalytically active D2 domain, while dEC contains a deletion between aa 20-142 corresponding to the extracellular domain of the wildtype PTPRA insert.

Confocal Fluorescence Resonance Energy Transfer Imaging

Ptpra KO mouse FLS (mFLS) were directly plated onto coverslips and allowed to grow to confluence in a 24 well plate. Cells were transfected once they had reached 90% confluency and starved for 12 h 36 h post transfection as described above. After starvation, a scratch wound was induced by drawing a micropipette tip through the middle of the coverslip. The wound was allowed to close for 12 h in high serum media (20% FBS) before cell fixation with 4% paraformaldehyde. The cells were then permeabilized by 0.2% triton-X and stained with primary, secondary, and direct conjugate antibodies. The coverslips were then mounted onto slides with molecular probe gold reagent. All images were acquired by our collaborator, Dr. William Kiosses, at the La Jolla Institute for Immunology.

Wound Healing Functional Assay

PTPRA KO mFLS were plated into 6 well plates and were allowed to grow to 90% confluence before transfection as described above. Cells were starved for 12 h 36 h post transfection, and a scratch wound was induced by drawing a micropipette tip through the middle of the coverslip. Pictures of the wound were acquired and the distance between the scratch margins marked to constitute the 0h timepoint. The wound was allowed to heal for 24 h in high serum media (20% FBS) before another set of pictures of the same wound was acquired constituting the 24h timepoint. Samples were then fixed and stained with crystal violet and differences between timepoints scored for each sample in ImageJ. Cells were visualized using a Motic AE2000 microscope at 4x

magnification. Each scratch wound was scored at four separate locations. Data was analyzed using the Kruskal-Wallis test with two tailed Mann-Whitney post-hoc test.

Crystal Violet Protocol

Cells were first fixed with prechilled methanol (-80 °C) for 10 minutes, then stained with 0.5% crystal violet in 25% methanol for 10 minutes. Cells were then rinsed and imaged.

Transwell Migration Functional Assay

Confluent FLS were harvested by light trypsin digestion and seeded at 2.5 x 10^4 cells in 100 microL serum-free DMEM containing 0.5% BSA in the upper chamber of a 6.5 mm-diameter Transwell polycarbonate culture insert (Costar) with a pore size of 8 microns. Inserts were placed in 24-well plates with 600 microL DMEM containing 5% FBS. The assay plates were incubated for 4 h, after which the Transwell inserts were removed and the upper chamber gently wiped with a cotton swab to remove non-migrating cells. Transwell membranes were fixed for 10 min in prechilled methanol and stained for 10 min in 0.5% crystal violet in 25% methanol. Cells were visualized using a Motic AE2000 microscope at 10x. Cell migration was quantified by counting 4 random fields. Data was analyzed using the Kruskal-Wallis test with two tailed Mann-Whitney post-hoc test.

Software

Zen Black was used to separate confocal multi images to separate images for further processing and analysis. Image pro-premier was used to quantify FRET data on

processed images through manual division of cells into four 60-120 degree quadrants, with quadrant 1 representing the lamellipodia containing the leading edge facing the induced scratch wound and quadrant 4 being directly opposite quadrant 1, and thus containing the lagging edge. ImageJ was used to process images for FRET analysis, and to quantify the results of functional assays. Data was analyzed using the Kruskal-Wallis test with two tailed Mann-Whitney post-hoc test.

Results

PTPRA dimerizes and localizes along the leading edge of PTPRA KO mFLS migrating towards an induced scratch wound (Figs. 3 & 4)

PTPRA KO mFLS were transfected with both FLAG and HA tagged versions of a wildtype, P210/P211L, dD2, or dEC PTPRA construct before a scratch wound was induced to promote their migration along the wound's edge. PTPRA-HA and PTPRA-FLAG both primarily localized at the leading edge of migrating cells. Cells for FRET studies were selected among the ones expressing relatively equal expression of FLAG and HA based on the intensity of emission of the respective fluorophors and FRET was acquired through excitation at 488 nm and collection at 568 nm. Areas of high FRET signal (represented in yellow/red in the calibrated FRET images) were found along the leading edge of the fixed and stained wild type (WT) cells suggesting that PTPRA dimers occur in FLS and also localize at the leading edge of migratory FLS. A qualitative morphologic assessment of the different constructs' phenotypes revealed a disruption in the continuity of the leading edge of P210/P211L and dD2-transfected cells and the creation of multiple lamellipodia in the dEC- transfected cells. Furthermore, FRET signal seemed to accumulate in "hotspots" that were aligned as a continuous front along the lamellipodia in WT and dEC-transfected cells, while the hotspots were disjointed, and focally distributed along the lamellipodia in cells transfected with P210/P211L and dD2 constructs.

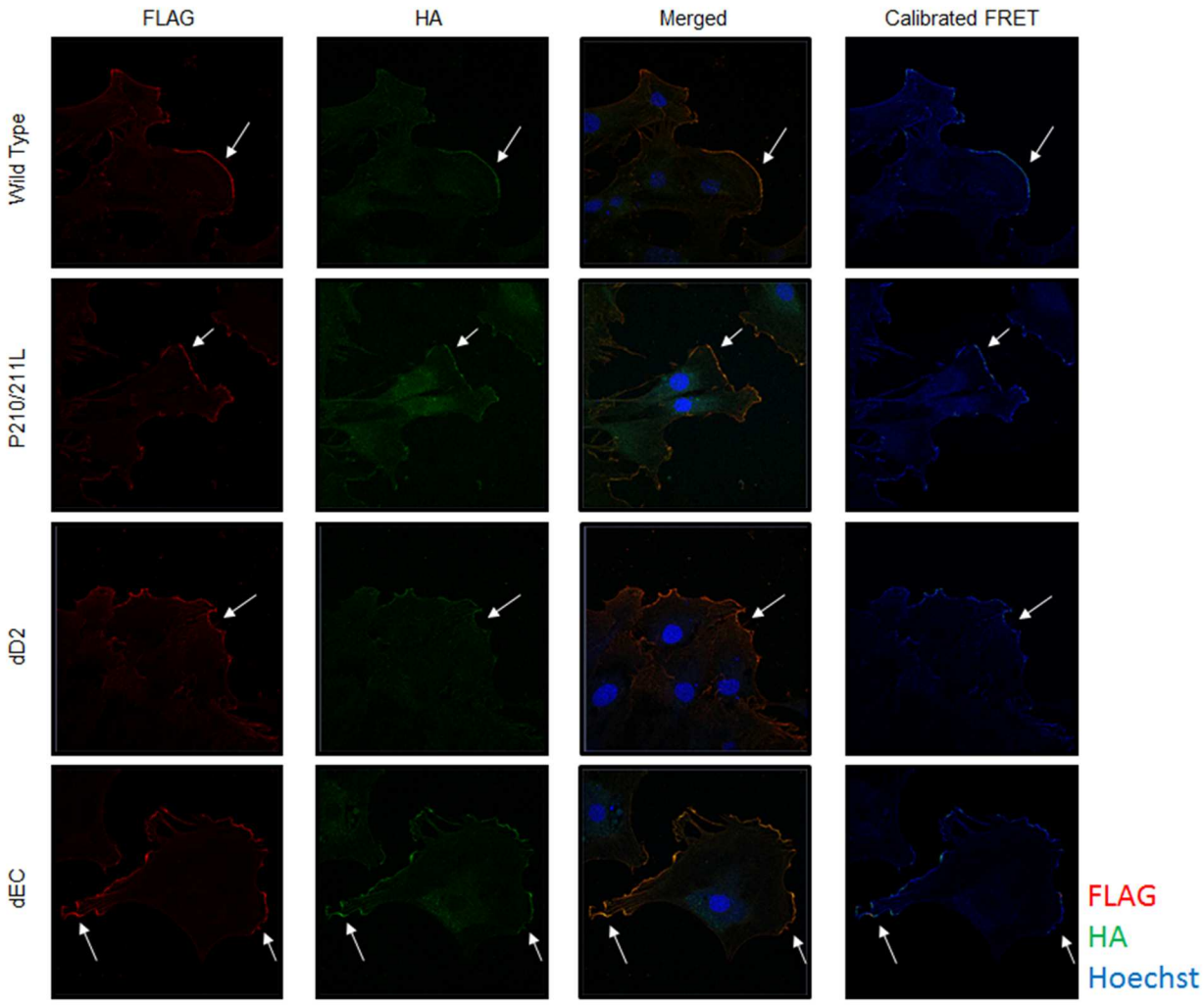

Figure 3. PTPRA localizes at the leading edge in mFLS migrating toward an induced scratch wound. mFLS were transfected with both FLAG and HA tagged PTPRA WT or mutant constructs and imaged for FLAG (red), HA (green), Hoechst (blue in the merged column). FRET signal was collected at 568 nm after excitation at 488 nm and the acquired data were then processed to create a calibrated FLAG::HA FRET image, displayed as a heatmap with dark blue representing low FRET signal and red representing areas of high FRET signal. Images are representative of four independent experiments using four different KO cell lines. The leading edge(s) are identified with a white arrow.

Images of individual cells were then divided into four quadrants, each subjected to quantification of the level of FRET signal in arbitrary units. This analysis revealed decreased overall FRET signal in cells transfected with all the mutant constructs compared to WT PTPRA in the quadrant corresponding to the lamellipodia of the leading edge of the cell (facing the wound). We observed similar expression levels of PTPRA among all constructs as determined via examination of the fluorescence intensity profiles of acquired cells. Thus, the data suggest that PTPRA mutations considered might impair PTPRA dimerization along the FLS leading edge.

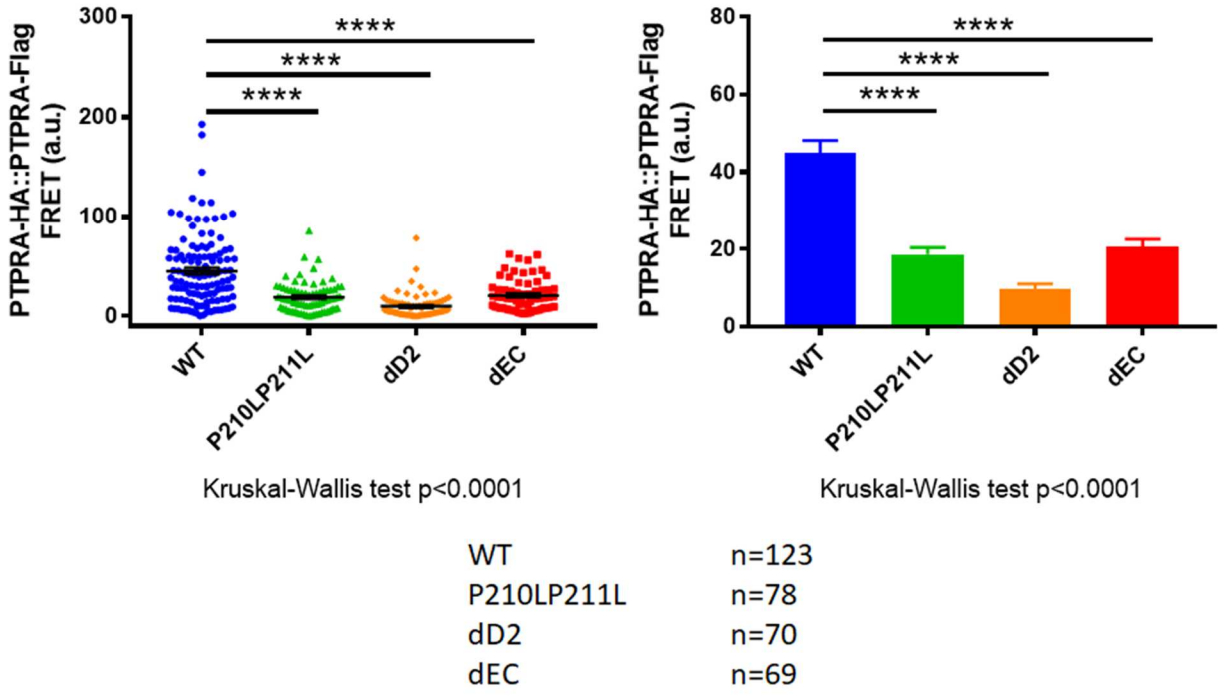

WT	n=123
P210LP211L	n=78
dD2	n=70
dEC	n=69

Figure 4. PTPRA dimerizes in mFLS at the leading edge of cells migrating toward an induced scratch wound. mFLS were transfected with both FLAG and HA tagged PTPRA WT or mutant constructs and then HA::FLAG FRET signal levels in the 90 degree quadrant corresponding to the leading edge of each cell (facing the wound) was measured. Data were pooled from four independent experiments using four different cell lines. Total number of cells analyzed for each construct is indicated below the graphs. Individual cells, each represented by a single point, for each mutant are shown in the graph on the left, while the aggregate mean and SEM of all cells for each mutant is displayed in the graph on the right. Mean±SEM are shown. Data was analyzed using the Kruskal-Wallis test with two tailed Mann-Whitney post-hoc test **** P<0.0001

PTPRA associates with Src along the leading edge of PTPRA KO mFLS migrating towards an induced scratch wound (Figs. 5 & 6)

After we collected FRET-based evidence of PTPRA dimerization along the leading edge of mFLS, my next objective was to study how PTPRA dimerization modulates its ability to interact with Src. A similar FRET-based experiment was performed, focused this time on the association between FLAG tagged PTPRA and endogenous Src, a well known PTPRA substrate that mediates PTPRA's control over the activation of the FAK pathway. The resulting images displayed a high concentration of Src along the leading edge of the lamellipodia of migrating cells, with overlap with FLAG-PTPRA in areas of high PTPRA expression. Calibrated FRET images revealed positive co-localization of PTPRA and Src within 10 nanometers distance. The cells' morphology and FRET patterns were similar to the previous experiment's results, with continuous FRET signals along the leading lamellipodia edge of WT transfectant mFLS, while a disrupted pattern with disjointed, isolated FRET hotspots was evident in lamellipodia of P210/P211L- and dD2-transfected cells, and FRET positive lamellipodia with a patter similar to WT transfected cells but expanding in multiple directions in dEC-transfected cells.

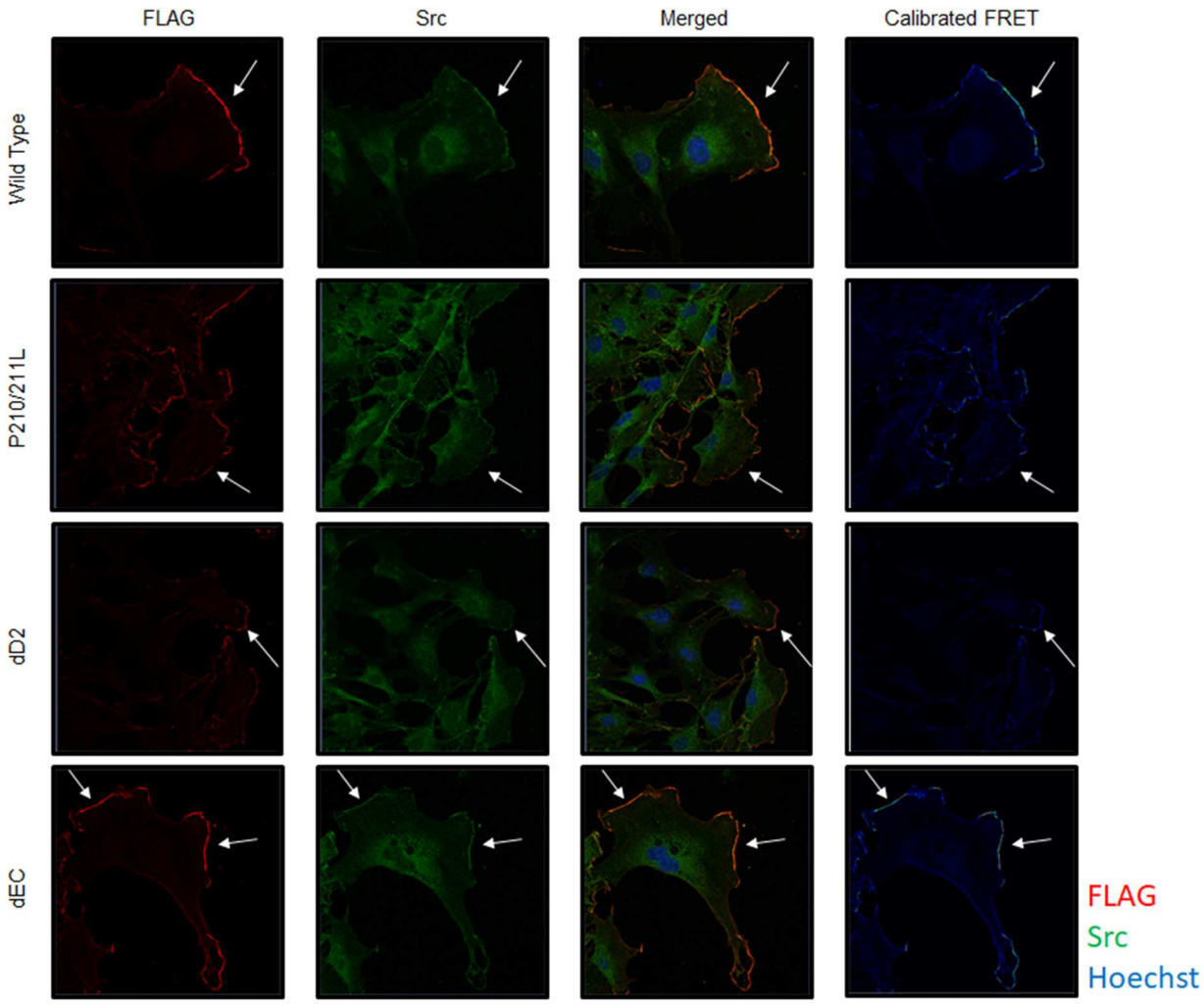

Figure 5. PTPRA associates with Src at the leading edge of mFLS migrating toward an induced scratch wound. mFLS were transfected with FLAG PTPRA WT or mutant constructs and then imaged for FLAG (red), Src (green), Hoechst (blue in the merged column). FRET signal was collected at 568 nm after excitation at 488 nm and the acquired data were then processed to create a calibrated FLAG::Src FRET image, displayed as a heatmap with dark blue representing low FRET signal and red representing areas of high FRET signal. Images are representative of four independent experiments using four different KO cell lines. The leading edge(s) are identified with a white arrow.

Images of individual cells were then divided into four quadrants, each subjected to quantification of the level of FRET in arbitrary units. All three mutant PTPRA constructs displayed significantly reduced FRET signal along the leading edge of migrating cells indicating impaired association of PTPRA with Src. This, when taken in conjunction with previous observations suggesting that the same PTPRA mutant constructs impaired PTPRA dimerization, suggest a model where -in apparent contrast with the canonical model or dimerization-induced transmembrane PTP inactivation- PTPRA displays increased association with Src and thus perhaps enhanced function in its dimeric state.

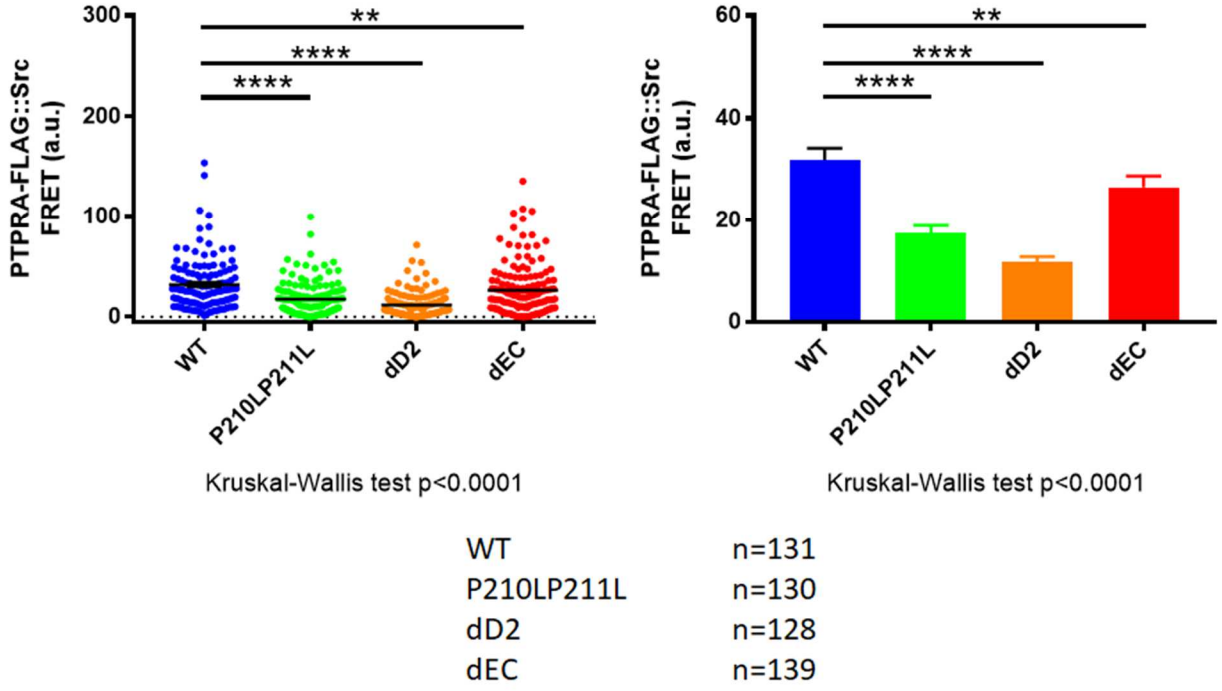

WT	n=131
P210LP211L	n=130
dD2	n=128
dEC	n=139

Figure 6. PTPRA associates with Src in mFLS at the leading edge of cells migrating toward an induced scratch wound. mFLS were transfected with FLAG tagged PTPRA WT or mutant constructs and then FLAG::Src FRET signal levels in the 90 degree quadrant corresponding to the leading edge of each cell (facing the wound) was measured. Data were pooled from four independent experiments using four different cell lines. Total number of cells analyzed for each construct is indicated below the graphs. Individual cells, each represented by a single point, for each mutant are displayed on the graph on the left, while the aggregate mean and SEM of all cells for each mutant is displayed on the graph on the right Mean±SEM are shown. Data was analyzed using the Kruskal-Wallis test with two tailed Mann-Whitney post-hoc test. **P<0.01, **** P<0.0001

PTPRA WT but not FRET-deficient/altered mutants can rescue the decreased rate of scratch wound closure of PTPRA KO mFLS

Since the previously shown FRET assays suggested that dimerization-deficient PTPRA also fails to associate with Src, a protein whose activation by PTPRA is necessary to promote cell motility, we next performed functional assays on PTPRA KO cells transfected with the same PTPRA constructs studied in FRET assays to see if the reduced motility of PTPRA KO mFLS could be rescued by dimerization-defective mutants of PTPRA. An assessment of induced scratch wound closure rates in

monolayers of PTPRA KO mFLS at 0 and 24 h revealed that transfection of PTPRA WT did enhance the rate of wound closure, but FLS transfected with any of the three dimerization-deficient mutant constructs of PTPRA (P210L/P211L, dD2 or dEC) displayed a significantly slower wound closure rate when compared to cells transfected with PTPRA WT.

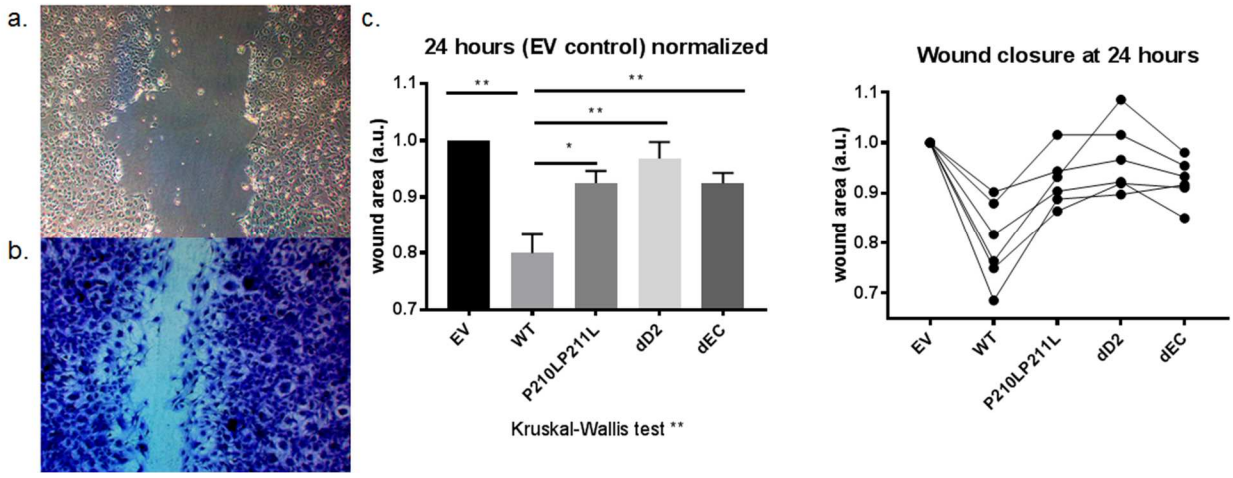

Figure 7. PTPRA WT but not dimerization-deficient mutants enhances mFLS scratch wound closure. mFLS were transfected with PTPRA WT or mutant constructs before a scratch wound was induced across the cell layer. The wound was then allowed to close for 24 h, after which cells were fixed and stained with crystal violet. a) Representative image of scratch wound of layer of mFLS transfected with PTPRA WT at 0 h b) Representative image of scratch wound of layer of mFLS transfected with PTPRA WT at 24 h stained with crystal violet c) Wound closure rates normalized to the rate of PTPRA KO mFLS transfected with empty vector (EV) control. Relative closure rates for each construct for each individual cell line are shown in the graph on the right, while the aggregate mean and SEM of all lines combined is shown in the graph on the left. Data was analyzed using the Kruskal-Wallis test with two tailed Mann-Whitney post-hoc test. Mean±SEM are shown. (n=6 cell lines) *P<0.05, ** P<0.01

PTPRA WT but not FRET-deficient/altered mutants can rescue the decreased migration rate of PTPRA KO mFLS across transwell membranes

In order to further confirm that WT PTPRA restores PTPRA function to a greater degree than mutant PTPRA constructs, we then performed a transwell migration assay

measuring FLS motility towards serum rich media as a chemotactic stimulus. Similar to as shown in the wound closure functional assay, FLS motility was rescued in the PTPRA WT-transfected cells, and a significantly increased number of cells traversing the membrane was observed for the WT-transfected cells when compared to dimerization-deficient mutant PTPRA-transfected cells.

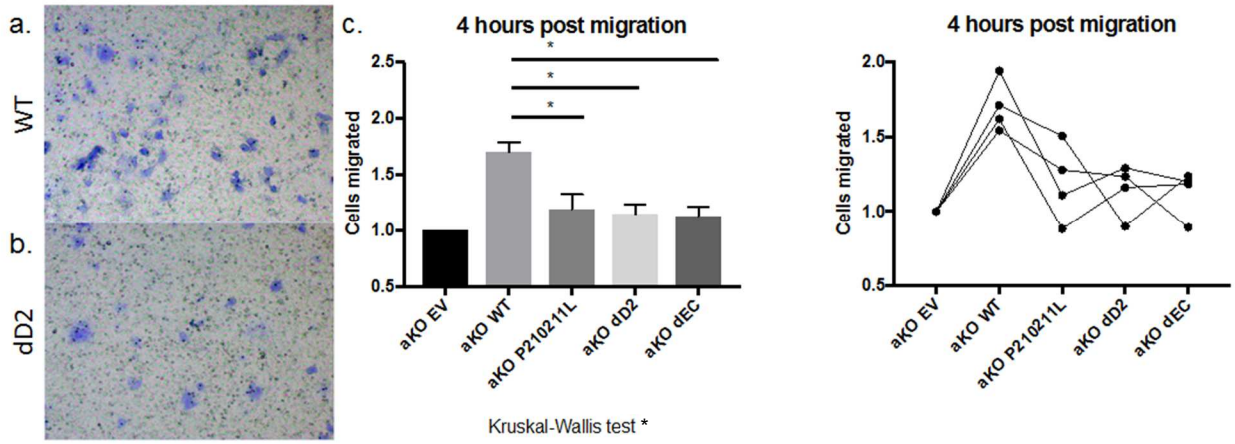

Figure 8. PTPRA WT but not dimerization-deficient mutants enhance mFLS migration across transwell membranes. mFLS were transfected with PTPRA WT or mutant constructs, before being counted and an equal number of cells being plated into transwell migration assay chambers. Cells were allowed to migrate for 4 h, after which they were fixed and stained with crystal violet. a) Representative transwell image of crystal violet stained mFLS transfected with PTPRA WT b) Representative transwell image of crystal violet stained mFLS transfected with dD2 mutant PTPRA c) Average cell count per 10x magnification transwell image per construct normalized to empty vector control (EV). Four images were acquired per construct for each cell line. Relative cell counts for each construct for each individual cell line are shown in the graph on the right, while the aggregate mean and SEM of all lines combined is shown in the graph on the left. Data was analyzed using the Kruskal-Wallis test with two tailed Mann-Whitney post-hoc test. Mean±SEM are shown. (n=4 cell lines) *P<0.05

Discussion

Positive correlation between PTPRA dimerization and PTPRA-Src association and function

FRET microscopy confirmed positive localization, dimerization, and association to Src of WT PTPRA at the leading edge of migrating FLS. WT PTPRA notably displayed increased rates of dimerization, association to Src, and functional rescue compared to all three mutant constructs assessed (P210L/P211L, dD2 and dEC). These results are difficult to reconcile with the canonical models of transmembrane PTP activation which states that phosphatase dimerization correlates with decrease function (Jiang, den Hertog, & Hunter, 2000).

The D2, wedge, and EC domains are necessary for proper PTPRA dimerization and function

The reduced PTPRA-FLAG::PTPRA-HA FRET signal in the leading edge quadrant of cells migrating towards an open scratch wound in the mutant constructs suggests that each one of the three domains considered (wedge, D2 and EC) might play a role in the dimerization of PTPRA at the leading edge.
PTPRA-P210/P211L and -dD2 appear to have impaired rates of dimerization, and when these mutations are introduced, PTPRA-FLAG and PTPRA-HA are still present at the leading edge of migrating FLS, however morphologically there is a failure to form coherent lamellipodia, and hot spots of FRET activity are bright, but small and discontinuous.

These qualitative cell morphology and FRET-dimerization observations correlated with an apparent decreased binding of PTPRA-P210L/P211L and -dD2 with Src at the leading edge, suggesting a model where the impaired formation of coherent lamellipodia at the leading edge of the cell towards the scratch wound is due to impaired dimerization of PTPRA, with results in decreased association with Src and downstream Src activation. Although we did not measure the phosphatase activity of the mutant constructs utilized, construct P210L/P211L is the canonical mutant which was utilized to impair PTPRA dimerization, and the two point mutations are not believed to affect the catalytically active cysteine residue in the D1 domain (which is responsible for most of the catalytic activity of PTPRA). dD2 also is not supposed to alter significantly the phosphatase activity of the D1 domain, although further experimentation is needed in order to prove that this is indeed the case.

PTPRA-dEC transfected cells showed a slightly different morphology from PTPRA-P210L/P211L and -dD2-transfected cells. Lamellipodia formation was apparently normal, however PTPRA-dEC-transfected cells often displayed multiple leading edges pointing to different directions. While the amount of FRET in the leading edge towards the wound in dEC-transfectants was reduced compared to WT-transfectants, our analysis excluded FRET signal located in the three non-leading edge quadrants of the cell. Thus, the total FRET signal per cell in dEC-transfectants might have been similar or higher than in WT- transfected samples, suggesting that the dEC mutant induces a possible loss in polarity of cell migration perhaps secondary to altered localization of PTPRA to the leading edge. Such loss of polarity rather than overall reduced Src activation could also explain the apparent impaired motility in the above-

mentioned functional assays. Thus, it is possible that the dEC mutant of PTPRA does not operate as a pure loss of function but with a more complex mechanism than the P210L/P211L and dD2 mutants. Further experimentation on PTPRA-dEC-transfected cells, including live FRET microscopy, is warranted in order to better characterize the functional role and mechanism of action of the EC domain.

Functional Assay Limitations

A limitation of the functional assays we performed in transfected cells at the population level is that PTPRA plasmid transfection efficiencies achieved with our method were about 20-25% when measured by flow cytometry of PTPRA KO mFLS (data not shown), and thus not all cells in the functional assay were transfected or expressed the proteins of interest. Nevertheless, the microscopy assays were performed on expressor cells and transfection of PTPRA WT rescued the phenotype of KO cells. Also, the change in wound closure rate or transwell migration numbers were found to be significant in the context of equal expression levels of all the constructs utilized as assessed by western blotting (data not shown).

Future direction

The next step to studying PTPRA dimerization and association with Src would likely involve the application of more recent FRET techniques and analysis, such as spectral, acceptor photobleach, superresolution, live, or fluorescence lifetime imaging microscopy analysis to confirm our sensitized emission FRET results (Ishikawa-Ankerhold, Ankerhold, & Drummen, 2012). Increasing transfection efficiency of our

plasmids would be desirable as it would enhance the robustness of our functional assays. Biochemical assays to verify the difference in activity of our mutant constructs could also prove useful in supporting our current working model.

Conclusion

Our confocal FRET analysis suggests that PTPRA dimerizes and localizes at the leading edge of migrating mFLS, and that PTPRA dimerization is positively correlated with the association of PTPRA with Src at the leading edge. These findings were consistent with functional assays, where dimerization deficient PTPRA constructs showing reduced Src interaction also displayed impaired ability to enhance mFLS motility. The same dimerization-deficient PTPRA mutants also induced an abnormal lamellipodia morphology as observed in microscopy assays. Our data are in line with previous data suggesting that the wedge, D2 domain, and EC domains of PTPRA are necessary for the dimerization of PTPRA and influence the functional activity of PTPRA. However, the discovery that dimerization upregulates PTPRA interaction with Src and correlates with increased motility-promotion function seems to be inconsistent with the canonical model of transmembrane PTP activation that postulates dimerized, inactive and monomeric, active states. Inhibitors of PTPRA are believed to be potentially useful as a new treatment option for RA in order to attenuate the invasive phenotype of RA FLS. Further work to elucidate the details of PTPRA dimerization and the exact role of each domain in such process might unravel molecular mechanisms that can be leveraged in order to accomplish PTPRA inhibition for therapeutic purposes.

References

Bottini, N., & Firestein, G. S. (2013). Duality of fibroblast-like synoviocytes in RA: passive responders and imprinted aggressors. *Nat Rev Rheumatol, 9*(1), 24-33. doi:10.1038/nrrheum.2012.190

Herrera Abreu, M. T., Penton, P. C., Kwok, V., Vachon, E., Shalloway, D., Vidali, L., Lee, W., McCulloch, C. A., & Downey, G. P. (2008). Tyrosine phosphatase PTPalpha regulates focal adhesion remodeling through Rac1 activation. *Am J Physiol Cell Physiol, 294*(4), C931-944. doi:10.1152/ajpcell.00359.2007

Humby, F., Bombardieri, M., Manzo, A., Kelly, S., Blades, M. C., Kirkham, B., Spencer, J., & Pitzalis, C. (2009). Ectopic lymphoid structures support ongoing production of class-switched autoantibodies in rheumatoid synovium. *PLoS Med, 6*(1), e1. doi:10.1371/journal.pmed.0060001

Ishikawa-Ankerhold, H. C., Ankerhold, R., & Drummen, G. P. (2012). Advanced fluorescence microscopy techniques--FRAP, FLIP, FLAP, FRET and FLIM. Molecules (Basel, Switzerland), 17(4), 4047–4132. doi:10.3390/molecules17044047

Jiang, G., den Hertog, J., & Hunter, T. (2000). Receptor-like protein tyrosine phosphatase alpha homodimerizes on the cell surface. *Mol Cell Biol, 20*(16), 5917-5929. doi:10.1128/mcb.20.16.5917-5929.2000

Myasoedova, E., Crowson, C. S., Kremers, H. M., Therneau, T. M., & Gabriel, S. E. (2010). Is the incidence of rheumatoid arthritis rising?: results from Olmsted County, Minnesota, 1955-2007. Arthritis and rheumatism, 62(6), 1576–1582. doi:10.1002/art.27425

Rubbert-Roth, A., & Finckh, A. (2009). Treatment options in patients with rheumatoid arthritis failing initial TNF inhibitor therapy: a critical review. Arthritis Research & Therapy, 11(Suppl 1). doi: 10.1186/ar2666

Shrestha, D., Jenei, A., Nagy, P., Vereb, G., & Szöllősi, J. (2015). Understanding FRET as a research tool for cellular studies. International journal of molecular sciences, 16(4), 6718–6756. doi:10.3390/ijms16046718

Smolen, J. S., Aletaha, D., & McInnes, I. B. (2016). Rheumatoid arthritis. The Lancet, 388(10055), 2023–2038. http://doi.org/10.1016/S0140-6736(16)30173-8

Stanford, S. M., Svensson, M. N., Sacchetti, C., Pilo, C. A., Wu, D. J., Kiosses, W. B., Hellvard, A., Bergum, B., Muench, G. R., Elly, C., Liu, Y. C., den Hertog, J., Elson, A., Sap, J., Mydel, P., Boyle, D. L., Corr, M., Firestein, G. S., & Bottini, N. (2016). Receptor Protein Tyrosine Phosphatase alpha-Mediated Enhancement of

Rheumatoid Synovial Fibroblast Signaling and Promotion of Arthritis in Mice. *Arthritis Rheumatol, 68*(2), 359-369. doi:10.1002/art.39442

Tertoolen, L. G., Blanchetot, C., Jiang, G., Overvoorde, J., Gadella, T. W., Jr., Hunter, T., & den Hertog, J. (2001). Dimerization of receptor protein-tyrosine phosphatase alpha in living cells. *BMC Cell Biol, 2*, 8. doi:10.1186/1471-2121-2-8

Tonks, N. K. (2006). Protein tyrosine phosphatases: from genes, to function, to disease. *Nat Rev Mol Cell Biol, 7*(11), 833-846. doi:10.1038/nrm2039

van der Wijk, T., Blanchetot, C., Overvoorde, J., & den Hertog, J. (2003). Redox-regulated rotational coupling of receptor protein-tyrosine phosphatase alpha dimers. *J Biol Chem, 278*(16), 13968-13974. doi:10.1074/jbc.M300632200